Bulletin of Engineering Geology and the Environment (2021) 80:4111–4124
https://doi.org/10.1007/s10064-021-02185-7

ORIGINAL PAPER

A sustainable landfill liner material: clay-fly ash geopolymers

Elmira Khaksar Najafi[1] · Reza Jamshidi Chenari[1] · Meghdad Payan[1] · Mahyar Arabani[1]

Received: 2 September 2020 / Accepted: 5 March 2021 / Published online: 13 March 2021

Abstract

Geopolymers offer a number of benefits, including high sorption capacity, sufficient durability, and substantial mechanical strength as well as low CO_2 emission and limited drying shrinkage, which may make them sustainable candidates to be utilized as landfill liner materials. Hence, this research is aimed at evaluating how a clay-fly ash geopolymer can meet the requirements proposed for mineral liners so as to compensate for the scarcity of suitable local clay. In this study, clay-fly ash geopolymers are synthesized from the mixtures containing 60% fly ash to the total solid mass and then activated by 10 M NaOH solutions. Several experiments are conducted to assess the mechanical strength, permeability, durability, and sorption capacity of the proposed liner material. Results depict that geopolymerzation has led to a prominent alteration in clay structure, contributing to a non-plastic soil with lower swelling potential and desiccation cracking probability. Proven to enhance sorption capacity and resist freeze-thaw cycles, the clay-fly ash geopolymers are shown to satisfy the criteria of volume shrinkage < 4%, permeability $\leq 1\times10^{-7}$ cm/s, unconfined compressive strength > 200 kPa, and plasticity index < 7–10. Microstructural analyses also corroborate that the binding agents result in the formation of coagulated particles covered by aluminosilicate gels, thus rendering a more sustainable material. Additionally, the sorption capacity of the clay-fly ash geopolymers exposed to freeze-thaw cycles also shows comparable values to the unexposed specimens.

Keywords Landfill liner · Durability · Permeability · Sorption capacity · Clay-fly ash geopolymers

Introduction

Landfilling is a prevalent and effective method of hazardous waste disposal. Compacted clay layers have been widely employed in landfills to simultaneously serve as impervious and chemical attenuating liners. Given that the mineral liners cannot remain impermeable to leachate in the long run, the amendment of their attenuation ability seems to be indispensable as even small municipal landfills may notably impact the groundwater quality. In addition to having sufficiently high impermeability and contaminant retention, liner materials are expected to effectively withstand mechanical and environmental stresses with minimum loss in their long time serviceability (Daniel 1993).

For hazardous waste, the hydraulic conductivity of liner materials must remain lower than 10^{-7} cm/s. To meet this criteria, compacted clay liners must have intrinsic properties of minimum fines content > 20–30%, gravel content < 30%, plasticity index < 7–10%, and maximum particle size < 25–50 mm (Daniel 1993; EC 1999/37/EC). In many cases, the unavailability of suitable local clays with such properties is itself a great concern. On the other side of the spectrum, for compacted clay layers, low hydraulic conductivity is parallel to high-plasticity index, which, in turn, may reduce the long-term serviceability owing to the increased seepage of leachate as a result of the consolidation phenomenon and drying shrinkage. Various consequences of freezing, e.g., vertical desiccation cracking, might also increase the hydraulic conductivity by as much as 1000 times, thus threatening the serviceability of liner (Daniel 1984; Sterpi 2015). Moreover, for a layer constructed of a high-plasticity clay, the diffusion of chemical components within its matrix may lead to an increase in the hydraulic conductivity of the liner. This is

✉ Reza Jamshidi Chenari
Jamshidi_reza@guilan.ac.ir

Elmira Khaksar Najafi
Elmirakhaksar@phd.guilan.ac.ir

Meghdad Payan
Payan@guilan.ac.ir

Mahyar Arabani
Arabani@guilan.ac.ir

[1] Department of Civil Engineering, Faculty of Engineering, University of Guilan, Guilan, Rasht, Iran

primarily due to the reduced double-layer thickness induced by variations in cation charges and the electrolyte concentration of pore solution (Broderick and Daniel 1990). Furthermore, macro-fabric fissures within a clay layer decrease the proper contact between the leachate and soil, thus reducing the attenuation capacity of the liner, offered by adsorption and cation exchange reactions (Bagchi 1987).

Due to the negative aspects associated with the scarcity of suitable local soils satisfying the above-mentioned requirements, different mineral mixtures treated with cement and lime have been exploited in geotechnical engineering practice. Nonetheless, their deficiencies in long-term durability and sacrificial mechanism of immobilization (Ganjian et al. 2004), as well as their negative environmental and financial downsides associated with the use of Portland cement and lime have prompted the introduction of alternative binders such as geopolymers (McLellan et al. 2011).

Geopolymers, produced by the alkaline activation of aluminosilicate resources such as clay and fly ash, seem to have rectified these concerns and have recently gained considerable attention for soil stabilization due to their excellent properties, including proper short-term strength, considerable chemical durability, sufficient freeze-thaw resistance, limited shrinkage, and low swelling potential (Pacheco-Torgal et al. 2015; Pourakbar et al. 2015; Rios et al. 2016; Alastair et al. 2018; Abdeldjouad et al. 2019). Sargent et al. (2013) used alkaline activation to enhance the mechanical properties and durability of soft alluvial soils against wetting-drying and freeze-thaw cycles. Fly ash-based geopolymers have also shown high resistance against freeze-thaw cycles and swelling (Bakharev 2005; Fu et al. 2011). A 30% decrease in the resistance of alkaline-activated fly ash binders was observed after 150 freeze-thaw cycles (Dolezal et al. 2007). Ma and Ye (2015) confirmed that early-age cracking due to drying shrinkage was not observed in the fly ash-based geopolymers. Alkaline activation, furthermore, significantly enhances the sorption capacity of fly ash due to the increased negatively charged sites and cation exchange reactions and therefore has been extensively employed for heavy metal removal from aqueous solutions throughout the literature (Engelhardt and Michel 1987; Wang et al. 2007; Al-Zboon et al. 2011; Zhang and Liu 2013; Muzek et al. 2014; Javadian et al. 2015). Thus, it seems that a clay-fly ash geopolymer is a low-energy technique for the design of an environmentally friendly landfill liner using available local clay, which can guarantee the long-term performance of an active-passive liner (Khaksar Najafi et al. 2020). However, geopolymerization has not been investigated widely in the design of active-passive liners in landfill sites.

Compacted clay is the primary constituent of all types of landfill liners, including compacted clay liners and geosynthetic clay liners (GCL). Therefore, the performance of compacted clay, as the active-passive component, is effectual in the functionality of the whole liner of any type. For this reason, the primary objective of this study is to propose a clay-fly ash geopolymer to be replaced by the compacted clay all over the liner so as to increase its efficiency, as the improved performance of the compacted clay liner by the geopolymerization process will be very effective in the efficacy of the whole liner layer.

In this context, the present study is to examine how effectively a clay-fly ash geopolymer can fulfill the minimum required properties to design an active-passive liner in comparison to an untreated clay. Samples containing 60% fly ash and 40% clay are activated by 10 M NaOH solutions to synthesize clay-fly ash geopolymers. A series of laboratory tests are conducted to evaluate the performance of the proposed liner material. Mechanical strength and stiffness are evaluated via unconfined compressive strength and indirect tensile strength tests, whereas hydraulic permeability is assessed by constant head experiments. Drying shrinkage, freeze-thaw effects and Atterberg limits of the specimens are attentively studied to examine their durability. Sorption capacity is also evaluated by several batch experiments. In addition, several microstructural analyses are also conducted on the clay-fly ash geopolymers and untreated clay so as to detect the imposed changes in micromechanical features formed by geopolymerization.

Materials and methods

Materials used

Clay

The used clay was collected from the sediments behind the Manjil dam located in Guilan Province in the north of Iran. This soil is medium-plasticity clay (CL) in accordance with ASTM D2487 (2000). The physical properties and the chemical compositions of the soil measured by energy-dispersive X-ray fluorescence (EDXRF) analysis are as listed in Table 1.

Fly ash

Fly ash used in this study was supplied by the electric power plant in India (DIRK). The chemical compositions of the fly ash, presented in Table 1, show that it is classified as a class F fly ash, a low-calcium precursor, based on ASTM C618 (2012). Its specific surface area, determined by the BET-nitrogen adsorption method, was measured to be equal to 4 m^2/g.

Aqueous solution

Aqueous solution was prepared to simulate the generated leachate in the experiments. It contained 100 and 200 mg/L

Table 1 Physical properties and chemical components (wt%) obtained from EDXRF analysis of the used soil and fly ash

Physical properties			Chemical components %		
Soil				Soil	Fly ash
	Values	Standard	SiO_2	50.1	60.8
Clay content (%)	33.69	ASTM D422 (2002)	Al_2O_3	12.9	28.3
Liquid limit (%)	36.80	ASTM D4318 (2000)	Fe_2O_3	6.39	3.27
Plastic limit (%)	19.60	ASTM D4318 (2000)	CaO	9.35	1.92
Specific gravity (Gs)	2.717	ASTM D854 (2014)	Na_2O	1.04	0.17
Maximum dry density (g/cm^3)	1.77	ASTM D698 (2007)	K_2O	2.54	0.76
Optimum water content (%)	19.00	ASTM D698 (2007)	MgO	3.62	0.61
			Others	13.95	4.03

of $Pb(SO_4)$ and zinc nitrate $Zn(NO_3)_2$ corresponding to 68.32 and 69.08 mg/L of Pb(II) and Zn(II), respectively.

Sample preparation

In a separate study conducted by the authors, a typical clay-fly ash geopolymer, namely CF6N10, containing 60% fly ash activated by 10 M NaOH resulting in an activator/fly ash ratio of 0.355, was observed to possess the highest adsorption capacity. Accordingly, to fabricate the specimens in the present study, the clay dried at 110 °C was initially mixed with 60% fly ash to obtain fairly homogeneous mixtures. Thereafter, the activator was added to the mixture so that uniform pastes with approximately 21.28% activator content were acquired. To synthesize clay-fly ash geopolymers and untreated clay specimens, compaction conditions were considered to be compatible with the state of 95% of the optimum moisture contents (OMC) for the corresponding mixtures obtained by the standard Proctor test (ASTM D698 2007). Accordingly, the target dry densities of 1.57 g/cm^3 and 1.75 g/cm^3 were measured for the two mixtures of "40% clay + 60% fly ash" and "100% clay", respectively.

Experimental approach

Hydraulic conductivity

The permeability of the untreated clay and clay-fly ash geopolymer to water and the aqueous solution, i.e., K_{vw} and K_{vaq} respectively, was measured according to ASTM D5856 (2002). The pastes were placed in cylindrical molds, 100 mm in diameter and 170 mm in height, and then compacted at a constant rate to reach the target dry densities. Molds containing clay-fly ash geopolymers were then placed at room temperature, 24 °C, and after 7 days of curing, were subjected to constant head flow provided separately by water and the aqueous solution. The apparent porosity of the tested samples was also determined in accordance with ASTM C20 (2000).

Unconfined compressive strength

Unconfined compressive strength (UCS) tests were carried out in accordance with ASTM D2166 (2000). UCS values were measured in two identical specimens, and the average experimental results were reported. A displacement-control soil-test CT-742 machine, fitted with a 133-kN-load cell and operating at a loading rate of 0.6 mm/min, was utilized for UCS tests to assess the uniaxial stress-strain response of geopolymers.

The specimens were prepared promptly after the above-mentioned mixing procedure. The pastes were placed in a cylindrical mold, 38 mm in diameter and 76 mm in height, and compacted with a constant rate to reach the target dry densities. Then, the specimens were removed and promptly wrapped in a plastic bag to prevent moisture loss. Afterwards, the samples were placed at room temperature, 24 °C, for different curing periods of 7 and 28 days.

Indirect tensile strength

The indirect tensile strength (ITS) tests were carried out based on ASTM D3379 (1975). Similar to the specimens prepared for UCS tests, cylindrical specimens, 76 mm in length and 38 mm in diameter, were used for ITS experiments. The tests were conducted on the untreated clay and CF6N10 cured for 28 days under a monotonic loading rate of 0.6 mm/min to determine peak tensile forces. According to the peak forces obtained, the ITS values were calculated using Eq. (1).

$$\mathrm{ITS} = \alpha \frac{2P}{\pi DL} \tag{1}$$

where P is the maximum load applied, D and L are the diameter and length of the sample, respectively, and α is the shape parameter, which can be calculated as $\alpha = 0.2621k + 1$, where $k = L/D$ (Abdeldjouad et al. 2019).

Atterberg limits

Liquid limit (LL) and plastic limit (PL) of the specimens were also measured in accordance with ASTM D4318 (2000). In order to evaluate the immediate and long-term effects of alkaline activation on the Atterberg limits of the treated clay, the corresponding limits were measured both immediately after mixing and also after 28 days of curing at the room temperature (24 °C).

Freeze-thaw cycles

Freeze-thaw cycle tests were conducted in accordance with ASTM D560 (2003) so as to determine the samples' resistance to weight loss for the full respective cycles. The pastes were compacted to reach the target dry densities in a cylindrical mold, 38 mm in diameter and 76 mm in height. For CF6N10, the first freeze-thaw cycle exposure occurred at the age of 28 days. A single freeze-thaw cycle consisted of approximately 24 h of freezing in a freezer set at −20±1°C followed by 24 h of thawing at room temperature.

Volume shrinkage

Shrinkage limit of the untreated clay and volume shrinkage of the untreated clay and clay-fly ash geopolymers were all measured according to ASTM D4943 (2002) to evaluate the cracking likelihood, which controls the long-term serviceability of a liner material.

Batch experiments

The prepared homogeneous pastes were placed in the cylindrical molds, 38 mm in diameter and 10 mm in height, resulting in the specimens with a constant area to thickness ratios of 11.33 cm^2/cm, and then compacted to achieve the target dry densities. Afterwards, the samples were removed and wrapped in plastic bags so as to prevent moisture loss and then cured at room temperature (24 °C). Following specific curing periods, the samples were removed from the plastic bags and except their top surfaces, coated with wax, and submerged in aqueous solutions. Additionally, the effects of different curing times, i.e., 7, 14, and 28 days, and various numbers of exposures to freeze-thaw cycles, i.e., 1 and 3 cycles, on the sorption capacity of clay-fly ash geopolymers were rigorously examined. After the batch experiments, the solutions were filtered, and the concentrations of Pb(II) and Zn(II) in solutions were determined by an atomic adsorption spectrometer. The removal efficiency and the equilibrium adsorption capacity (q_e) for Pb(II) and Zn(II) are defined as follows:

$$\text{Removal efficiency}\ (\%) = \frac{(C_0 - C_e)}{C_0} \times 100 \quad (2)$$

$$q_e(mg/g) = \frac{(C_0 - C_e)}{W} \times V \quad (3)$$

where C_0 and C_e are, respectively, the initial and equilibrium concentrations of Pb(II) and Zn(II) ions in the solution (mg/L), V is the volume of solution (L), and W is the weight of an adsorbent (g).

Microstructural analysis

The surface morphology of the untreated clay and clay-fly ash geopolymers cured for 7 and 28 days was evaluated by SEM/EDS analyses using a MIRA III instrument. Their powder had been coated with a thin layer of gold in a sputter coater before the measurements were performed. SEM images were also utilized to analyze the morphology of untreated clay and clay-fly ash geopolymers cured for 7 days after undergoing three freeze-thaw cycles.

The X-ray diffraction (XRD) patterns of the clay, fly ash, and clay-fly ash geopolymers at the age of 7 days were analyzed with a Pan Analytical Xpert Pro diffractometer (PW1730). The operating conditions were 40 kV and 30 mA. The radioactive source was Cu generating a wavelength equal to 1.54056 Å. The step size and time per step used were equal to 0.5° and 1 s, respectively.

Fourier transform infrared (FTIR) spectra of the untreated clay and clay-fly ash geopolymers cured for 7 days, unexposed and exposed to freeze-thaw cycles, and 28 days were studied using an FTIR device (AVATAR) with an attenuated total reflectance (ATR) unit in the range of 4000–400 cm^{-1}.

The specific surface area, pore size distribution, and total pore volumes of the untreated clay and clay-fly ash geopolymers cured for 7 days were measured from N_2 gas adsorption-desorption isotherms at the temperature of liquid nitrogen (−196 °C) by BELSORP MINI II instrument. The specific surface area was calculated in accordance with the Brunauer-Emmett-Teller (BET) equation (Wang et al. 2007; Luukkonen et al. 2016). Pore size distributions were obtained from desorption data using the Barrett-Joyner-Halenda (BJH) method (Luukkonen et al. 2016).

Results and discussion

Hydraulic conductivity

The results obtained from the permeability tests illustrate that the K_{vw} of the untreated clay and CF6N10 cured for 7 days were 2.04 $\times 10^{-6}$ cm/s and 5.19 $\times 10^{-8}$ cm/s, respectively. These K_{vw} values of both samples are observed to be higher than their corresponding K_{vaq} values, which were 7.35 $\times 10^{-7}$

cm/s and 4.84 $\times 10^{-8}$ cm/s for untreated clay and CF6N10, respectively. The permeability of the untreated clay to water and the aqueous solution is nearly thirty-eight and fifteen times as much as those measured for CF6N10, respectively. K_{vw} and K_{vaq} values of CF6N10 cured for 7 days satisfy the required limit of hydraulic conductivity. In general, fly ash-based binders show low hydraulic conductivity due to the very small pore sizes (Pacheco-Torgal et al. 2015). Compatible with the obtained results, a mixture of 20% bentonite-fly ash was reported by Mollamahmutoglu and Yilmaz (2001) to meet the permeability criterion for a liner material. Sivapullaiah and Moghal (2011) also indicated that adding 10–20% bentonite, gypsum, or lime to fly ash caused the hydraulic conductivity of the liner to reduce to less than 10^{-9} m/s.

Saturated hydraulic conductivity is primarily influenced by the pore features of soil as well as the viscosity and density of fluid (Mitchell 1976). Having higher apparent porosity, 35% compared to 31.8%, the untreated clay is more permeable to water compared to the measured value for CF6N10. Several reasons may contribute to the lower permeability of CF6N10. Most importantly, the growth of amorphous geopolymeric products filling the porosity of the treated clay leads to an overall decrease in the pore space, accompanied by a general decrease in hydraulic conductivity to water compared to that of the untreated clay. Furthermore, geopolymerization changes the fabric of the treated soil due to the formation of geopolymeric gels, causing the disaggregated grains to connect and form coagulated particles quite similar to small clods and consequently reducing the water flow at particle level (Benson and Daniel 1990; Glukhovsky 1994; Sivapullaiah and Baig 2011).

Concerning the permeability to the aqueous solution, for low-plasticity clay, hydraulic conductivity decreases with the increased concentration of salt solution. The contaminant solution decreases the double-layer thickness and contributes to the edge-to-face flocculated fabric of the clay. The properties of high-plasticity clay and low-plasticity clay are mostly controlled by double-layer thickness and its fabric, respectively (Sargent et al. 2013). The aqueous solution, possessing a lower dielectric constant and higher electrolyte and cation concentration compared to distilled water, has reduced repulsive forces in micro and mesopores. This feature substantially contributes to the edge-to-face flocculated fabric of clay with smaller clods and consequently a decrease in hydraulic conductivity (Benson and Daniel 1990; Rao and Mathew 1995; Yilmaz et al. 2008; Gupta et al. 2011). Benson and Daniel (1990) also reported decreases as much as four to six orders of magnitude in hydraulic conductivities of soils with smaller clods. According to SEM analyses, the clay-fly ash geopolymers consist of a large number of finer clusters, rendering a flocculated fabric, leading to a decreased permeability. Furthermore, Li et al. (2013) reported that the permeability of kaolin, a low-plasticity clay, increased by 16.7% when permeated with less concentrated Ca solutions (1 and 5 mM), while its value was about 10 times lower than the original value for the solution containing 10 Mm. Jo et al. (2005) also showed that the strong electrolyte leads to a decrease in the permeability of geosynthetic clay liner compared to that reported for lower electrolyte.

In comparison to the exchangeable cations and pore salt concentration, the dielectric constant of pore solution has profound effect on the above-mentioned alteration in clay fabric (Mitchell 1976). Given the lower dielectric constant of aqueous solution compared to water, it commonly leads to the flocculated fabric with small clods. For CF6N10, geopolymerization has mainly converted the clay structure to a cementitious one which is not affected by the properties of aqueous solution. This may be the main reason why the aqueous solution has reduced the permeability of CF6N10 considerably less than that of the untreated clay.

Strength and stiffness

Figure 1a and b present the stress-strain curves obtained from the UCS and ITS tests of the untreated clay and CF6N10. It is evident that the clay-fly ash geopolymers possess considerably higher UCS and ITS values compared to the untreated clay, which could satisfactorily meet the UCS > 200 kPa criterion for compacted landfill liner material (Kolawole et al. 2006). Murmu et al. (2019) also reported that the compressive strength of a mixture of expansive clay and 20% fly ash enhanced to 2500 kPa after 28 days of curing time, which was more than ten times the reported strength for the untreated clay.

According to Fig. 1a, although the clay-fly ash geopolymers exhibit brittle behavior with sudden drops at their failure strains, the slopes of the ascending branches increase considerably, contributing to the significant increase in their stiffness with smaller failure strains compared to the untreated soil. This is further pronounced for the clay-fly ash specimens cured for 28 days, referring to the formation of more aluminosilicate gels. Similarly, Pourakber et al. (2015) reported that the geopolymerization resulted in brittle post-peak behavior along with smaller failure strain, contributing to lower settlements in the liner constructed by the proposed material.

Figure 1b illustrates that alkaline activation has changed the post-peak behavior, causing the maximum ITS value and the failure tensile strain to increase substantially. The failure strain of CF6N10 has enhanced to 0.016, approximately three times that of the untreated clay, 0.0054. This rise in the failure strain and maximum ITS value is of significant importance as the repair of tensile cracks formed as a result of differential settlements is impossible (Daniel 1993). Ergo, higher ITS

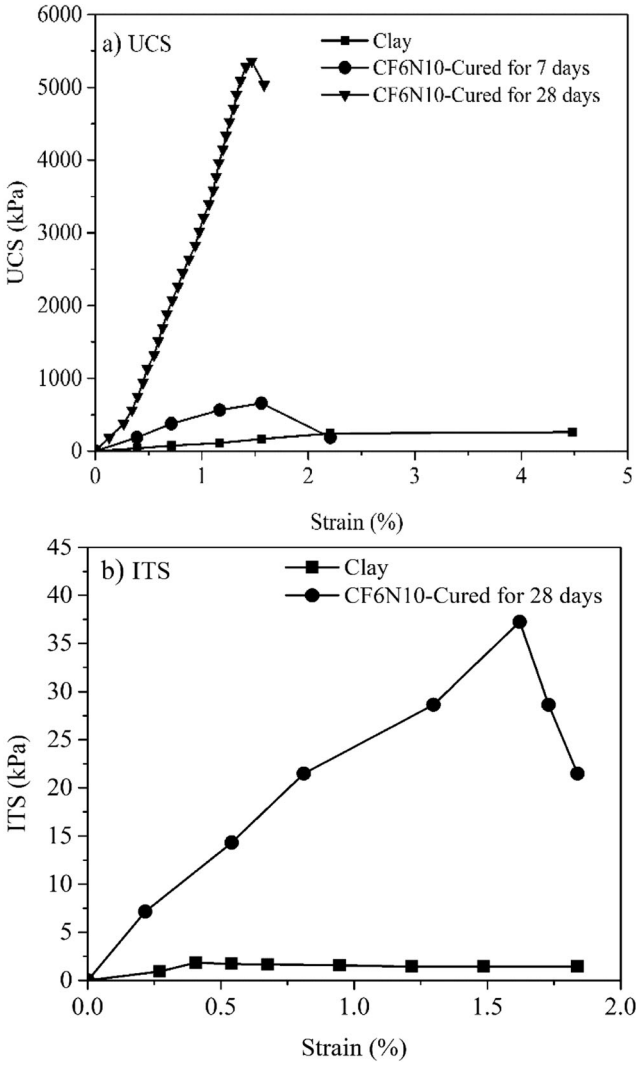

Fig. 1 The mechanical strengths of the untreated clay and CF6N10 cured at room temperature. **a** UCS and **b** ITS

value associated with larger failure strain helps enhance the long-term serviceability of the liner material.

Durability

Atterberg limits

The results reveal that the alkaline activation considerably reduces the immediate LL and PL values of clay to 19.30% and 15.50%, respectively, resulting in a plasticity index of < 7–10%. Moreover, it means that the compaction process of the clay-fly ash geopolymer is more feasible than that of the untreated clay with higher LL value. More importantly, increasing the curing time to 28 days caused the treated clay to thoroughly lose its plasticity. In good agreement with the obtained results in the course of this study, Murmu et al. (2019) also found that LL and PL of an expansive clay treated with alkaline activation of fly ash decreased after a curing period of 28 days, so that the specimens turned out to be completely non-plastic. Given that the general behavior of clays, such as swelling and consolidation probability, is predominantly controlled by their plasticity, CF6N10 shows considerably lower swelling and consolidation likelihood, thus enhancing the long-term durability and consequently the operating service time of a liner.

It is accepted that the lower dielectric constant of NaOH (i.e., 57.5), compared to that of water (i.e., 80), along with the increased electrolyte concentration and cation valence causes a reduction in the diffuse double-layer thickness and turn the clay structure into a flocculated fabric with larger internal void spaces for water entrapment. Although the corresponding phenomenon consequently leads to the increased LL values for low-plasticity clays (Mitchell 1976; Sridharan et al. 1988; Sridharan 2014), the high portion of fly ash in CF6N10 has contributed to a considerable reduction in its immediate LL value. In good agreement with the obtained results, for a mixture of soil and fly ash, Ahmed (2014) showed that increasing fly ash content from zero to 20% caused a reduction in the liquid limit, and thus, the plastic index.

Regarding the long-term LL and PL values of CF6N10, geopolymerization process profoundly affects the fabric of clay-fly ash geopolymers, so that the increased curing period contributes to a significant drop in LL and PL values, leading to a sort of non-plastic materials. In this context, Glukhovsky (1994) introduced the processes of destruction-coagulation, coagulation-condensation, and condensation-crystallization as the main mechanisms for the alkaline activation reactions. In the second stage, the inter-connection of the disaggregated products gives rise to polycondensation and consequently constitution of coagulated particles. Palomo et al. (2004) also proposed that alkaline activation at the ambient temperature leads to aluminosilicate gels with short-range ordered aluminosilicate gels surrounding the clay particles. Thus, it seems that alkaline activation changes the clay fabric due to very fact that the clay particles are covered by geopolymeric gels, resulting in coagulated grains. These coarser fractions behave like silt (Arasan and Yetimoglu 2008) and become non-plastic in long run. To endorse the results obtained, Provis and van Deventer (2009) also described sodium aluminosilicate hydrate gels as a charge-balanced aluminosilicate structure which was observed to decrease the water adsorption tendency and consequently reduce the plasticity properties.

Volume shrinkage

The volume shrinkage values measured for the untreated clay and CF6N10 were equal to 8.7% and 2.4%, respectively. It is evident that CF6N10 can efficiently satisfy the threshold limit of 4% to mitigate the volume shrinkage of a mineral liner (Ganjian et al. 2004; Kolawole et al. 2006). In agreement with the obtained results, Khadka et al. (2018) found that alkaline

activation of clay containing 12% fly ash showed the best results so as to control the shrinkage behavior of expansive soils. Furthermore, according to the results found by Ahmed (2014), lower plastic index contributes to reduced volume shrinkage. Murmu et al. (2019) also showed that the shrinkage limit of treated expansive clay decreased to almost zero for fly ash content more than 10%.

As can be observed in Fig. 2, the untreated clay with the shrinkage limit equal to 13.08% is quite vulnerable to severe cracking when it dries at room temperature, whereas the clay-fly ash geopolymer has not considerably suffered from desiccation cracking. It is well proved that shrinkage plays an important role in liners' performance due to the likelihood of cracking in a restrained condition. Indeed, the durability and permeability of liners might suffer from fractures mainly caused by drying shrinkage and differential settlement (Daniel 1993; Sterpi 2015).

The results confirm the observations obtained from Atterberg limits tests, where the behavior of the treated clay has been significantly affected by geopolymerizaton. Drying shrinkage in geopolymers is related to the micro-crack formation due to the loss of water. The track of the unit weight of the clay-fly ash geopolymers cured for 7 and 28 days show a decrease from 2.04 to 2.01 g/cm^3, which may be attributed to the micro-crack formation (Lee and Lee 2013). Moreover, the coagulated particles resulting from geopolymerization may be another reason for lower shrinkage in CF6N10, because it has been well corroborated that flocculated fabric leads to a considerably lower weight loss caused by drying shrinkage compared to the dispersed structure with parallel-oriented particles (Mitchell 1976).

Freeze-thaw cycles

Freeze-thaw cycles tests aimed to determine the resistance of liner martial to weight loss due to being exposed to the sequential freeze-thaw cycles. The results presented in Fig. 3 demonstrate that the untreated clay has shown more weight loss, in the range of 5.53 to 11.91%, during the corresponding freeze-thaw cycles. For clay-fly ash geopolymer, losses in weight are in the range of 4.62 to 6.73%, where the significant reduction in weight could be observed to occur during the first three cycles and further cycles have solely contributed to slight weight losses with no surface cracking. Similarly, Arora and Aydilek (2005) found that the clay containing 40% fly ash and 7% lime has a 6.8% loss in weight after 12 freeze-thaw cycles. Parsons and Milburn (2003) also reported that the weight loss in fly ash-treated clay was in the range of 7 to 19% after 12 freeze-thaw cycles.

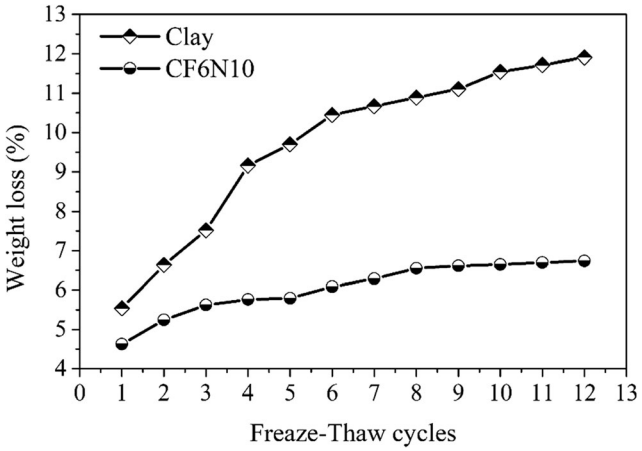

Fig. 3 Weight loss experienced during sequential freeze-thaw cycles for the untreated clay and CF6N10

Due to ice pressure within the pores, soil exposed to freeze-thaw cycles suffers from particle separation on a microscopic scale (Arora and Aydilek 2005), giving rise to a reduction in the overall weight of specimens. The untreated clay is more vulnerable to weight loss due to having higher porosity and water content as well as weaker inter-particle bonding, which could be significantly improved by geopolymerization.

Although the freezing process affects only shallow layers, compacted clay liners are vulnerable to freezing-induced damage either during construction or on their side slopes (Daniel 1993). Additionally, previous studies showed that when it comes to dense soils, such as compacted liner material,

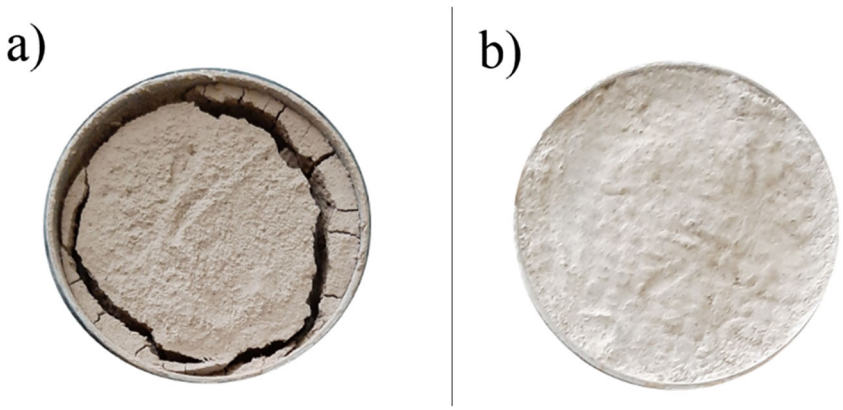

Fig. 2 Cracking patterns of **a** the untreated clay and **b** CF6N10 cured at room temperature

freeze-thaw cycles would be more critical, causing weak soil structure and increased permeability (Qi et al. 2008). All results obtained, admit the great efficiency of CF6N10, as a landfill liner material, in resisting freeze-thaw cycles.

Sorption capacity

Sorption performance

Table 2 shows the results of the batch experiments for the untreated clay and clay-fly ash geopolymer. As could be observed, the clay-fly ash geopolymer, CF6N10, synthesized and cured for 7 days at the ambient temperature (24 °C), has improved Pb(II) and Zn(II) removal compared to the untreated clay, especially in the case of Pb(II), where the removal efficiency has enhanced from 8.32 to 95%. Similarly, Sahoo et al. (2013) observed that alkali modified fly ash with 1 M NaOH solution, after keeping at 90°C for 24 h, exhibited 92% and 94% efficiency for the removal of zinc and lead ions, respectively, from acid mine drainage.

Using the unwashed wax-coated adsorbents, the pH of the solutions has raised from 4.3 to 8.2 during the batch experiments after 90 min of contact time. Since the precipitations of Pb(II) and Zn(II) require the pH value as minimum as 8.5–9 and 8.7–9.6, respectively, heavy metal extraction by clay-fly ash geopolymers was conceivable to occur through the aforementioned adsorption process (Abdullah et al. 1999; Pang et al. 2009; Brbooti et al. 2011).

In comparison to the untreated clay, alkaline activation has increased the sorption capacity due to several reasons. First, it leads to the increase in the negatively charged surfaces due to $Si(O_4)^{4-}$ tetrahedrons replacement by $Al(O_4)^{5-}$ tetrahedrons, which could be neutralized by cations such as heavy metal ions. Besides, the heavy metals could be exchanged with Na ions through cation exchange reactions (Engelhardt and Michel 1987; Glukhovsky 1994; Wang et al. 2007; Lancellotti et al. 2013; Pacheco-Torgal et al. 2015). A geopolymer matrix is, furthermore, a favorable alkaline environment for the precipitation of metal ions in relatively insoluble forms (Ganjian et al. 2004; Bumanis et al. 2019).

Although the initial concentrations and valence capacity of Pb(II) and Zn(II) are identical, Zn(II), due to its lower ionic radius, has access to more adsorptive sites on the surface of the walls of the pores as well as higher tendency to replace the Na ions via cation exchange reactions (Mitchell 1976; Anirudhan and Suchithra 2008; Bumanis et al. 2019). In this regard, in a separate study, the authors found that it seems the apparent porosity of CF6N10 to be more important to the Pb(II) removal, while the Zn(II) sorption is mainly influenced by the active sites, including adsorption sites and cation exchangeability.

Further analyses of the sorption capacity, including breakthrough curves and diffusion coefficient, were out of scope of the current work, as these investigations need a separate thorough study to be discussed in detail. However, in a qualitative sense, the lower porosity and consequently the lower hydraulic conductivity of the proposed liner compared to that of the compacted clay liner justify its longer breakthrough time.

Effect of curing time

The results presented in Table 2 depict that the increase in the curing time from 7 to 14 and 28 days has contributed to the enhanced removal efficiency of Zn(II) and Pb(II), which is parallel to the reduction of the apparent porosity from 31.8 to 22.5% and 21.4%, respectively. The overall increase in curing time from 7 to 28 days has increased the Pb(II) and

Table 2 The results of the batch experiments for the untreated clay and clay-fly ash geopolymer

Specimens	Geopolymer dosage (g/L)	Curing time (days)	Moisture content (%)	Apparent porosity (%)	Freeze-thaw cycles	Removal efficiency (%)		q_e (mg/g)	
						Pb(II)	Zn(II)	Pb(II)	Zn(II)
Clay	329	-	18.00	35.0	-	8.32	72.5	0.025	0.152
CF6N10-7[a]	289	7	14.94	31.8	-	95.0	95.9	0.223	0.229
CF6N10-14[a]	289	14	-	22.5	-	96.1	96.4	0.226	0.230
CF6N10-28[a]	289	28	-	21.4	-	96.3	97.9	0.227	0.233
CF6N10-D[b]	289	7	Dry	31.8	-	85.8	96.0	0.202	0.229
CF6N10-S[b]	289	7	Saturated 16.20	31.8	-	94.1	95.9	0.222	0.229
CF6N10-1[c]	289	7	-	31.8	1	91.4	94.1	0.215	0.224
CF6N10-3[c]	289	7	-	31.8	3	94.7	95.9	0.223	0.229

[a] 7, 14, and 28: days of curing time

[b] D and S: moisture condition referring to dry and saturated states

[c] 1 and 3: number of freeze-thaw cycles

Zn(II) removal by 1.3% and 2% so as to reach 96.3% and 97.9%, respectively. As can be observed, an increased curing time of 7 to 14 days has worked better to enhance the Pb(II) removal compared to Zn(II) removal, while the further increase in curing time to 28 days has performed better for Zn(II) removal. All in all, the highest sorption capacity observed for CF6N10-28 may be attributed to the more aluminosilicate gels formed as a result of the prolonged curing time (Pacheco-Torgal et al. 2015), which is in good agreement with the significant rise in the mechanical strength of the treated clay cured for 28 days in comparison to that of the specimen cured for 7 days (Fig. 1a). Similarly, Wang et al. (1994) and Haha et al. (2011) reported that the pore sizes and volumes continuously decrease due to the prolonged curing time. The lower porosity of CF6N10-28 has contributed to a lower increase of the adsorption for Pb(II) as compared to Zn(II). The increased active sites, nonetheless, improved the overall removal efficiencies of Pb(II) and Zn(II).

Effect of moisture conditions

According to the test data presented in Table 2, both dry and saturated specimens show similar sorption capacities for Zn(II) removal, whereas the Pb(II) removal by CF6N10-D is 8.3% lower than CF6N10-S. This observation may be attributed to the different mechanisms involved in their sorption process. As Zn(II) ions have smaller ionic radius compared to Pb(II), they can simply occupy the active sites close to the surfaces. However, Pb(II) ions have to diffuse to get access to active sites, referring to the dominated effect of adsorbent pores on the Pb(II) removal. The predominant influence of diffusivity on Pb(II) removal has made a reduction in sorption capacity of dry specimens, as the absence of moisture in the pores of adsorbents has limited the accessibility of Pb(II) to active sites due to the diffusion of reduced solutes (Melkior et al. 2005 and 2007; Gimmi and Kosakowski 2011). Given that there is no clear difference between sorption capacities of CF6N10 and CF6N10-S, it may mean that the moisture condition in CF6N10 is near to saturation, although saturated specimens contributed to slightly lower Pb(II) removal. It seems that the increased leachate velocity within the adsorbent has reduced the contact time required for completing the sorption mechanisms in saturated conditions (Bagchi 1987).

Effect of freeze-thaw cycles

The results illustrate that CF6N10-3 exposed to 3 freeze-thaw cycles has shown higher removal efficiency for both heavy metals compared to that obtained for CF6N10-1 exposed to only 1 freeze-thaw cycle. Therefore, the sorptions of Pb(II) and Zn(II) by CF6N10-3 are close to those for the unexposed treated clay. It means that 3 cycles of freezing and thawing have not resulted in adverse effects on the sorption capacity of the treated clay (CF6N10). Once again, both specimens exposed to freeze-thaw cycles have worked better for Zn(II) removal, especially the specimen experiencing 1 freeze-thaw cycle (CF6N10-1), as the removal of Zn(II) by CF6N10-1 is 2.7% more than that of Pb(II). However, the sorption by CF6N10-3 has shown a higher rise in Pb(II) removal increased by 3.3% in comparison to a 1.8% rise observed for Zn(II) removal. Compatible with the results reported by Du et al. (2020), freeze-thaw cycles could be observed to substantially enhance the sorption of Pb(II).

It seems that the surfaces of soil particles are augmented as a result of freezing which breaks down the soil grains (Hinman 1970; Bullock et al. 1988; Oztas and Fayetorbay 2003), contributing to the more adsorption sites and finer particles with more inter-particle pores. The results obtained from SEM analyses also reveal that the freezing process has broken the clay particles. Furthermore, the FTIR results show higher peaks in the positions referring to the Si-O stretching vibration which contributes to the smaller crystalline phases due to the crushing of soil particles. Although the freeze-thaw cycles resulted in a decrease in alkaline activation process which needs high temperature, the breakage of soil particles could compensate for the active sites, especially for 3 cycles of freezing and thawing.

Microstructural analysis

SEM/EDS

Figure 4a, b, and c exhibit the microstructural morphology of the untreated clay and CF6N10 cured for 7 and 28 days, respectively. Figure 4a shows the morphology of the untreated clay having flat surfaces and irregularly discrete shaped particles with flaky edges. Circular areas in Fig. 4b depict aluminosilicate gels for CF6N10 specimen at the age of 7 days and it is conspicuous from Fig. 4c that the increased curing time has led to the more dissolution of precursors, i.e., the portion of finer and adsorption sites, confirming the enhanced sorption capacity of specimens with prolonged curing time.

It is evident that the treated clays consist of a large number of finer clusters. Indeed, the clay particles have been covered with binding agents due to the formation of the aluminosilicate gels in the form of clusters, rendering a flocculated fabric of the treated clay (Davidovits and Comrie 1988; Xu and Van Deventer 2000).

Figure 5 reveals that the structures of the untreated clay and CF6N10 have been affected by freeze-thaw cycles due to the formation of the ice lenses which have notably contributed to the breakage of clay particles (Oztas and Fayetorbay 2003). In comparison to Fig. 4a, the layered structure of clay has

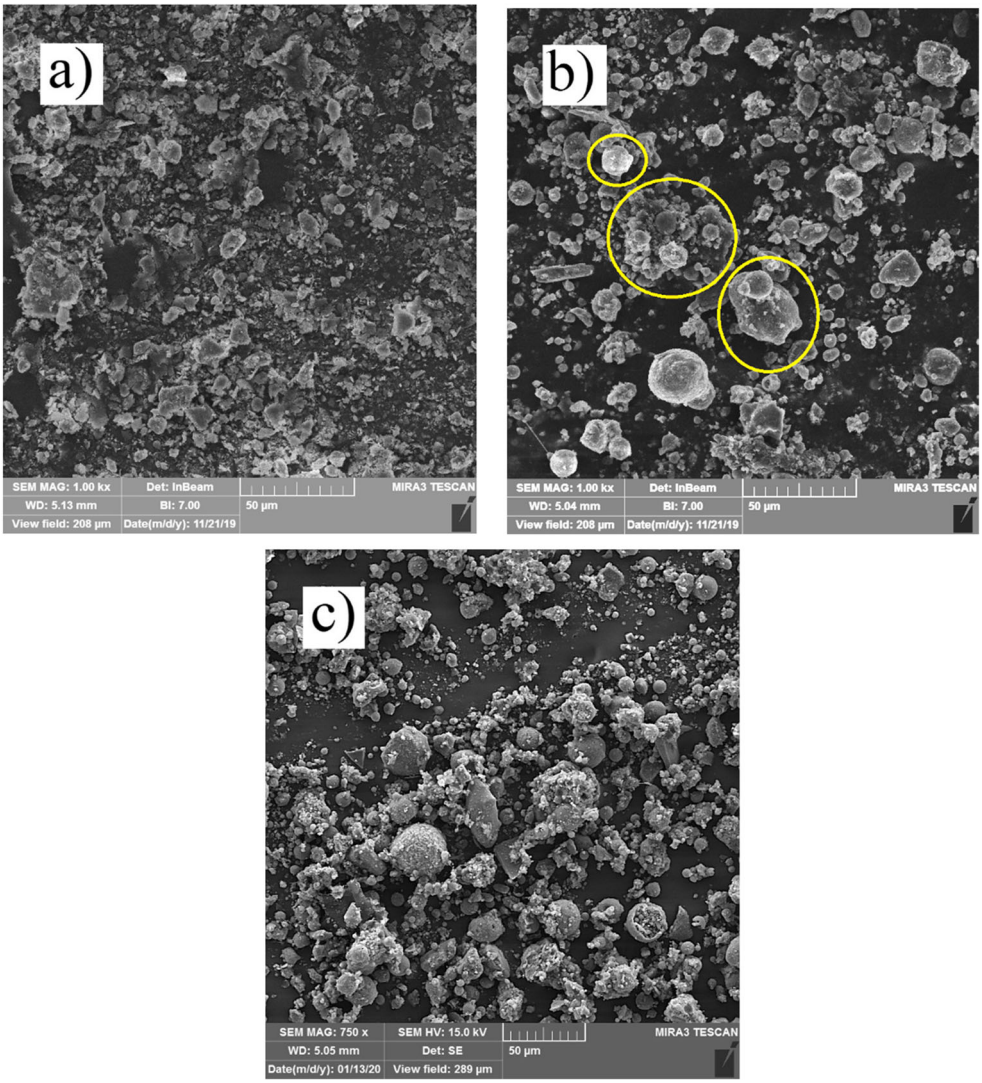

Fig. 4 SEM images of **a** the untreated clay, and the clay-fly ash geopolymer cured for **b** 7 and **b** 28 days

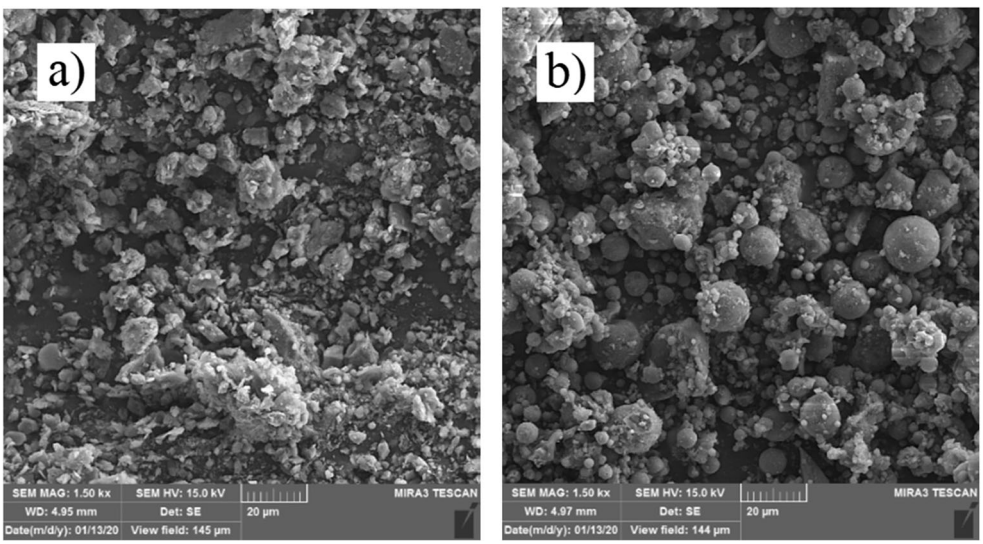

Fig. 5 SEM images of the specimens exposed to 3 freeze-thaw cycles **a** untreated clay and **b** CF6N10

disappeared in Fig. 5a, as the freezing process has broken the clay particles, confirming the observations made in the "Freeze-thaw cycles" section.

The chemical elements of CF6N10 after reaching the equilibrium adsorption were calculated from the average of 10 points measured using EDS line scan analyses. In comparison to the chemical elements of the raw materials presented in Table 1, after adsorption, Pb(II) and Zn(II) have been included in the elements of CF6N10, with the contents of 0.52 and 2.60 (wt.%), respectively. This observation confirms the extraction of heavy metals by the adsorption process rather than the hydroxide precipitation in the solution.

X-ray diffraction (XRD) analysis

Figure 6 exhibits the XRD patterns of the untreated clay, fly ash, and CF6N10 at the age of 7 days with major mineral phases identified. As can be seen, after a curing period of 7 days, the CF6N10 specimen has considerably lower crystalline phases compared to the used raw materials, so that the peaks detecting muscovite, clinochlore, and mullite are less intense and have transformed to sillimanite (Al_2SiO_5). This means that clinochlore and muscovite also participated in the alkaline activation process due to the disappearance of their corresponding reflections. Given that the dissolutions of muscovite [$KAl_2Si_3AlO_{10}(OH)_2$] and clinochlore [$(Mg, Fe)_6(Si, Al)_4O_{10}(OH)_8$] have released Mg, Fe, and K ions, a lower portion of clay in CF6N10 mitigated the competition between these released cations and Pb(II) and Zn(II) (Bumanis et al. 2019), thus confirming the higher sorption capacity of the treated clays due to the lower number of competitive cations to occupy the active sites.

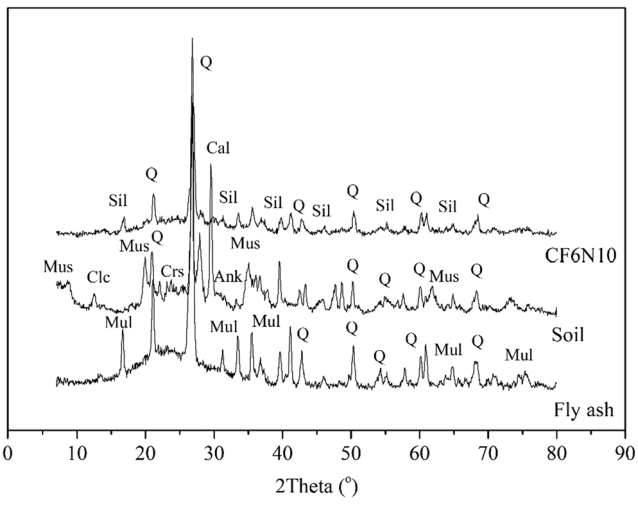

Fig. 6 XRD patterns of the untreated clay, fly ash, and CF6N10 at the age of 7 days with major mineral phases identified: Q, quartz; Mul, mullite; Mus, muscovite; Clc, clinochlore; Crs, cristobalite; Cal, calcite; Ank, ankerite; Sil, sillimanite

Fourier transform infrared (FTIR) spectroscopy

The FTIR spectra of the specimens of untreated clay and CF6N10 cured for 7 and 28 days are presented in Fig. 7. The increased curing time from 7 to 28 days has contributed to the shifts of about 2.55 cm^{-1} and 22 cm^{-1} in the bonds referring to Si-O stretching vibration (Madejova and Komadel 2001). Indeed, the bonds at 1033.2 cm^{-1} and 1438.86 cm^{-1} in the FTIR spectra of CF6N10 have reached 1030.65 cm^{-1} and 1416.64 cm^{-1} in the FTIR spectra of CF6N10-28, respectively. They refer to the lower Si–O–Si bonds due to their reorganization in the clay-fly ash geopolymer (Davidovits 2011). In the untreated clay, the frequencies at 3426 cm^{-1}, which is the sign of bending and stretching vibrations of (H–O–H), have shifted to the higher frequencies in CF6N10 cured for 7 and 28 days, referring to the transformation of the adsorbed water into the structural water of binding agents (Pacheco-Torgal et al. 2015). In the FTIR spectra of CF6N10, the disappearance of the peak in the feldspar region, i.e., frequencies between 720 and 500 cm^{-1}, also refers to the alkaline activation of the clay minerals (Madejova and Komadel 2001). The peak at 558.27 cm^{-1}, indicating Si–O–Al bonds with Al in octahedral coordination, has reduced to 543.85 cm^{-1} for CF6N10-28, denoting their dissolution and participation in geopolymerization as a result of increased curing time (Van Jaarsveld et al. 2002).

Regarding the effect of consecutive cycles of freezing and thawing on the FTIR results, the frequency at 1033.2 cm^{-1}, observed in the unexposed CF6N10, has slightly increased to 1035.15 cm^{-1} after 3 freeze-thaw cycles, referring to the smaller crystalline phases due to the breakdown of soil particles. For CF6N10-3, the frequencies at 3422.46 cm^{-1} have experienced a drop compared to that observed in the untreated clay, referring to the limited transformation of water into binding agents (Madejova and Komadel 2001). The FTIR results confirm the observations obtained for the batch experiments, where the reduction in the formation of aluminosilicate gels was compensated by the breakage of soil particles, as presented in Fig. 5b.

Specific surface area and pore features

The experimental results show that specific surface area and mean pore diameter of CF6N10 cured for 7 days are 17.88 m^2/g and 32.24 nm, respectively, while these values for the untreated clay are considerably lower, i.e., 6.047 m^2/g and 12.29 nm, respectively. This justifies the higher sorption capacity of CF6N10. The total pore volume of CF6N10 (0.0491 cm^3/g) is slightly lower than that of the untreated clay (0.0544 cm^3/g). The results also show that CF6N10 contains a lower portion of macro-pore volumes > 50 nm (0.0126) as compared to that of the untreated clay (0.0133), referring to the lower pore space for water flow and consequently smaller hydraulic conductivity.

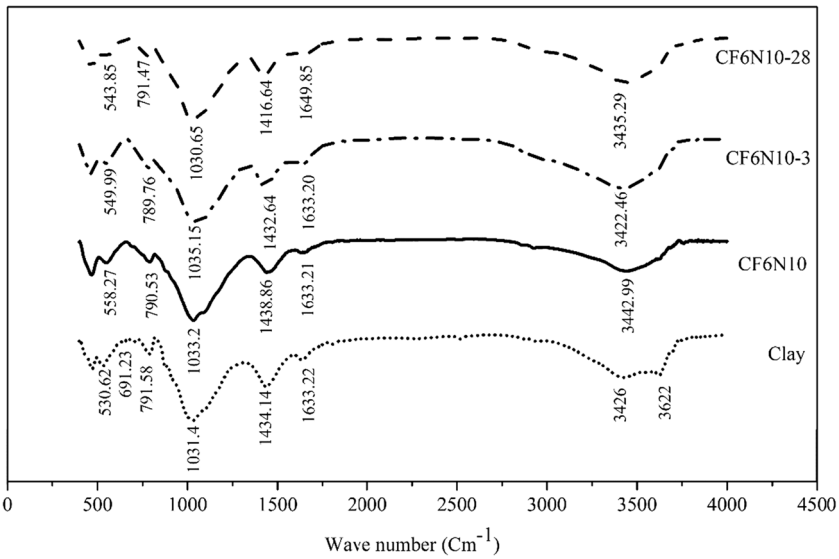

Fig. 7 FTIR spectra of the untreated clay and CF6N10, CF6N10-3, and CF6N10-28

Concluding remarks

This study aimed at taking the best advantage of geopolymerization so as to propose a clay-fly ash geopolymer as a sustainable active-passive liner material. To this end, the sorption capacity, mechanical strength, durability, and permeability of the untreated clay and clay-fly ash geopolymer were rigorously examined and compared. The observations not only corroborate the performance of the clay-fly ash geopolymers to fulfill the minimum requirements of a landfill liner material but also can guarantee their long-term serviceability due to the proportionate, profound consequential changes in the fabric and mechanical response of the treated clay. Indeed, geopolymerization converts the clayey soil to a non-plastic silt-like material due to the very fact that clay particles are covered by geopolymeric gels, hence forming coagulated particles, with a considerably lower likelihood of swelling, consolidation, and drying shrinkage. The higher maximum ITS value associated with the larger failure tensile strain of the clay-fly ash geopolymers could remarkably decrease the cracking likelihood related to the differential settlement. Furthermore, barely affected by either the moisture condition or freeze-thaw cycles, the proposed liner material exhibited higher sorption capacity as compared to the untreated clay. Regarding environmental factors, the clay-fly ash geopolymer showed a lower loss in weight due to the stronger bonds existing among its constituents induced by binding agents. Additionally, the prolonged curing time positively affected the mechanical properties and sorption capacity of the clay-fly ash geopolymer owing to the lower porosity and more aluminosilicate gels formed by alkaline activation process, thus making it a sustainable candidate to be employed as the landfill liner in future.

References

Abdeldjouad L, Asadi A, Ball RJ, Nahazanan H, Huat BH (2019) Application of alkali-activated palm oil fuel ash reinforced with glass fibers in soil stabilization. Soils Found 59:1552–1561

Abdullah SRS, Rahman RA, Mohamad AB, Mustafa MM, Khadum AAH (1999) Removal of mixed heavy metals by hydroxide precipitation. Kejuruteraan 11(2):85–101

Ahmed AG (2014) Fly ash utilization in soil stabilization Proceeding of International Conference on Civil. Biological and Environmental Engineering, Istanbul (Turkey)

Alastair M, Andrewa H, Pascaline P, Mark E, Pete W (2018) Alkali activation behavior of un-calcined montmorillonite and illite clay minerals. Appl. Clay Sci 166:250–261. https://doi.org/10.1016/j.clay.2018.09.011

Al-Zboon K, Al-Harahsheh MS, Bani Hani F (2011) Fly ash-based geopolymer for Pb removal from aqueous solution. J Hazard Mater 188:414–421. https://doi.org/10.1016/j.jhazmat.2011.01.133

Anirudhan TS, Suchithra PS (2008) Synthesis and characterization of tannin-immobilized hydrotalcite as a potential adsorbent of heavy metal ions in effluent treatments. Appl Clay Sci 42(1):214–223. https://doi.org/10.1016/j.clay.2007.12.002

Arasan S, Yetimoglu T (2008) Effect of inorganic salt solution on the consistency limits of two clays. Turkish J Eng EnvSci 32:107–115

Arora S, Aydilek AH (2005) Class F Fly-Ash-Amended Soils as Highway Base Materials. J. Mater. Civil. Eng 17(6)

ASTM C20 (2000) Standard test method for apparent porosity, water absorption, apparent specific gravity, and bulk density of burned refractory brick and shapes by boiling water

ASTM C618 (2012) Standard specification for coal fly ash and raw or calcined natural pozzolan for use in concrete. American Society for Testing and Materials, Book of Standards Vol. 04.02, West Conshohocken, PA

ASTM D2166 (2000) Standard test method for unconfined compressive strength of cohesive soil. Annual Book of ASTM standards
ASTM D2487 (2000) Standard classification of soils for engineering purposes (unified soil classification system). ASTM D2487, Annual Book of ASTM Standards, Soil and Rock, Section 4, 4
ASTM D3379 (1975) Tensile strength and Young's modulus for high-modulus single-filament materials. Annual Book of ASTM standards
ASTM D422 (2002) standard test method for particle-size analysis of soils. Annual Book of ASTM standards
ASTM D4318 (2000) Standard test methods for liquid limit, plastic limit, and plasticity index of soils. ASTM Annual Book of Standards, 4
ASTM D4943 (2002) Standard test method for shrinkage factors of soils by the wax method
ASTM D560 (2003) Standard test methods for freezing and thawing compacted soil-cement mixtures
ASTM D5856 (2002) Standard test methods for measurement of hydraulic conductivity of porous material using a rigid-wall, compaction-mold permeameter
ASTM D698 (2007) Standard test methods for laboratory compaction characteristics of soil using standard effort
ASTM D854 (2014) Standard test methods for specific gravity of soil solids by water pycnometer
Bagchi A (1987) Natural attenuation mechanisms of landfill leachate and effects of various factors on the mechanisms. Waste ManagRes 5: 453–463. https://doi.org/10.1177/0734242X8700500159
Bakharev T (2005) Durability of geopolymer materials in sodium and magnesium sulfate solutions. Cem Concr Res 35:1233–1246
Benson CH, Daniel DE (1990) Influence of clods on hydraulic conductivity of compacted clay. J Geotech Eng 116(8)
Brbooti MM, Abid BA, Al-Shuwaiki NM (2011) Removal of mixed heavy metals using chemicals precipitation. J Eng Technol 29(3): 595–612
Broderick GP, Daniel DE (1990) Stabilizing compacted clay against chemical attack. J Geotech Eng 116:1549–1567
Bullock MS, Kemper WD, Nelson SD (1988) Soil cohesion as affected by freezing, water content, time and tillage. Soil Sci Soc Am J 52(3): 770–776
Bumanis G, Novais RM, Carvalheiras J, Bajare D, Labrincha JA (2019) Metals removal from aqueous solutions by tailored porous waste-based granulated alkali-activated materials. Appl. Clay Sci 179. https://doi.org/10.1016/j.clay.2019.105147
Daniel DE (1984) Predicting hydraulic conductivity of clay liners. J Geotech Eng 110:285–300
Daniel DE (1993) Geotechnical practice for waste disposal. Springer Science Business, Media Dordrecht
Davidovits J (2011) Geopolymer chemistry and applications, 3rd edn. Institut Geopolymere, Saint-Quentin, France
Davidovits J, Comrie D (1988) Archaeological long-term durability of hazardous waste disposal: preliminary results with geopolymer technologies. Division of Environmental Chemistry, American
Dolezal J, Skvara F, Svoboda P, Sulc R, Kopecky L, Pavlasova S, Myskova L, Lucuk M, Dvoracek K (2007) Concrete based on fly ash geopolymers. In: Alkali activated materials – research, production and utilization 3rd conference. Prague, Czech Republic, pp 185–197
Du L, Dyck M, Shotyk W, He H, Lv J, Cuss CW, Bie J (2020) Lead immobilization processes in soils subjected to freeze-thaw cycles. Ecotoxicol Environ Saf 192:110–288
EC (1999) Council Directive 1999/31/EC of 26 April 1999 on the landfill of waste
Engelhardt G, Michel D (1987) High resolution solid state RMN of silicates and zeolites. John Wiley and Sons, New Delhi
Fu Y, Cai L, Wu Y (2011) Freeze–thaw cycle test and damage mechanics models of alkali-activated slag concrete. Constr Build Mater 25: 3144–3148
Ganjian E, Classie P, Tyrer M, Atkinson A (2004) Preliminary investigations into the use of secondary waste minerals as a novel cementitious landfill liner. Constr Build Mater 18:689–699. https://doi.org/10.1016/j.conbuildmat.2004.04.020
Gimmi T, Kosakowski G (2011) How mobile are sorbed cations in clays and clay rocks? Environ Sci Technol 45(4):1443–1449
Glukhovsky V (1994) Ancient, modern and future concretes, First Inter. Conf. Alkaline Cements and Concretes, Kiev, Ukraine, 1:1–8
Gupta V, Hampton MA, Stokes JR, Nguyen AV, Miller JV (2011) Particle interactions in kaolinite suspensions and corresponding aggregate structures. J. Colloid Interface Sci 359:95–103
Haha MB, Le Saout G, Winnefeld F, Lothenbach B (2011) Influence of activator type on hydration kinetics, hydrate assemblage and microstructural development of alkali activated blast-furnace slags. Cem Concr Res 41(3):301–310. https://doi.org/10.1016/j.cemconres.2010.11.016
Hinman WG (1970) Effects of freezing and thawing on some chemical properties of three soils. Can J Soil Sci 50(2):179–182
Javadian H, Ghorbani F, Tayebi HA, Hosseini SM (2015) Study of the adsorption of Cd (II) from aqueous solution using zeolite-based geopolymer, synthesized from coal fly ash: kinetic, isotherm and thermodynamic studies. Arab J Chem 8:837–849. https://doi.org/10.1016/j.arabjc.2013.02.018
Jo HY, Benson CH, Shackelford CD, Lee JM, Edil TB (2005) Long term hydraulic conductivity of a geosynthetic clay liner permeated with inorganic salt solutions. J Geo Geoenviro Eng 131:405–417
Khadka SD, Jayawickrama PW, Senadheera S (2018) Strength and shrink/swell behavior of highly plastic clay treated with geopolymer. Transp. Res. Rec 2672 (52)
Khaksar Najafi E, Jamshidi Chenari R and Arabani M (2020) The potential use of clay-fly ash geopolymer in the design of active-passive liners-review. Clay. Clay Miner https://doi.org/10.1007/s42860-020-00074-w In press
Kolawole J, Osinubi M, Nwaiwu CMO (2006) Design of compacted lateritic soil liners and covers. J Geotech Geoenviron 132(2):203–213
Lancellotti I, Ponzoni C, Barbieri L, Leonelli C (2013) Alkaline activation process for incinerator residues management. Waste Manag 33: 1740–1749. https://doi.org/10.1016/j.wasman.2013.04.013
Lee NK, Lee HK (2013) Setting and mechanical properties of alkali-activated fly ash/slag concrete manufactured at room temperature. Constr Build Mater 47:1201–1209
Li Z, Katsumi T, Inui T, Takai A (2013) Fabric effect on hydraulic conductivity of kaolin under different chemical and biochemical conditions, Soils. Found 53(5):680–691
Luukkonen T, Sarkkinen M, Kemppainen K, Ramo J, Lassi U (2016) Metakaolin geopolymer characterization and application for ammonium removal from aqueous solutions and landfill leachates. Appl. Clay Sci 119:266–276. https://doi.org/10.1016/j.clay.2015.10.027
Ma Y, Ye G (2015) The shrinkage of alkali activated fly ash. Cem Concer Res 68:75–82
Madejova J, Komadel P (2001) Baseline studies of the clay minerals society source clays: infrared methods. Clay. Clay Miner 49:410–432. https://doi.org/10.1346/CCMN.2001.0490508
McLellan BC, Williams RP, Lay J, van Riessen A, Corder GD (2011) Costs and carbon emissions for geopolymer pastes in comparison to Ordinary Portland Cement. J Clean Prod 19:1080–1090
Melkior T, Yahiaoui S, Motellier S, Thoby D, Tevissen E (2005) Cesium sorption and diffusion in Bure mudrock samples. Appl Clay Sci 29(3-4):172–186
Melkior T, Yahiaoui S, Thoby D, Motellier S, Barthes V (2007) Diffusion coefficients of alkaline cations in Bure mudrock. Phys Chem Earth 32(1-7):453–462
Mitchell JK (1976) Fundamentals of soil behavior. John Wiley and Sons, New York

Mollamahmutoglu M, Yilmaz Y (2001) Potential use of fly ash and Bentonite mixture as liner or cover at waste disposal areas. J Environ Geol 40:1316–1324

Murmu AL, Jain A, Patel A (2019) Mechanical properties of alkali activated fly ash geopolymer atabilized expansive clay. KSCE J Civ Eng 23(9):3875–3888

Muzek MN, Svilovic S, Zelic J (2014) Fly ash-based geopolymeric adsorbent for copper ion removal from waste water. Desalin Water Treat 52:2519–2526. https://doi.org/10.1080/19443994.2013.792015

Oztas T, Fayetorbay F (2003) Effect of freezing and thawing processes on soil aggregate stability. Catena 52(1):1–8. https://doi.org/10.1016/S0341-8162(02)00177-7

Pacheco-Torgal F, Labrincha JA, Leonelli C, Palomo A, Chindaprasirt P (2015) Handbook of Alkali activated cements, mortars and concretes. Publishing in Civil and Structural Engineering, Wood Head

Palomo A, Alonso S, Fernández-Jiménez A, Sobrados I, Sanz J (2004) Alkaline activation of fly ash: NMR study of the reaction products. J Am Ceram Soc 87:1141–1145

Pang FM, Teng SP, Teng TT, Omar AKM (2009) Heavy metals removal by hydroxide precipitation and coagulation-flocculation methods from aqueous solutions. Water Qual Res J 44(2):174–182. https://doi.org/10.2166/wqrj.2009.019

Parsons RL, Milburn JP (2003) Engineering behavior of stabilized soils. Proceeding of 82nd Annual Meeting, Transportation Research Board. Washington, DC 1837(1). https://doi.org/10.3141/1837-03

Pourakbar S, Asadi A, Huat BB, Fasihnikoutalab MH (2015) Soil stabilization with alkali-activated agro-waste. J Environ Geotech 2(6):359–370

Provis J, van Deventer JSJ (2009) Geopolymers: structure, processing, properties and industrial applications. Woodhead Publishing Limited, Cambridge

Qi J, Ma W, Song C (2008) Influence of freeze–thaw on engineering properties of a silty soil. Cold Reg SciTechnol 53:397–404

Rao SN, Mathew PK (1995) Effects of exchangeable cations on hydraulic conductivity of a marine clay. Clays. Clay Miner 43:433–437

Rios S, Cristelo C, Viana Da Fonseca A, Ferreira C (2016) Structural performance of alkali activated soil-ash versus soil-cement. J Mater Civ Eng 28(2)

Sahoo PK, Tripathy S, Panigrahi MKP, Equeenuddin SKMD (2013) Evaluation of the use of an alkali modified fly ash as a potential adsorbent for the removal of metals from acid mine drainage. Appl Water Sci 3:567–576

Sargent P, Hughes PN, Rouainia M, White ML (2013) The use of alkali activated waste binders in enhancing the mechanical properties and durability of soft alluvial soils. Eng Geol 152:96–108

Sivapullaiah PV, Baig MAA (2011) Gypsum treated fly ash as a liner for waste disposal facilities. Waste Manag 31:359–369

Sivapullaiah P, Moghal A (2011) Role of gypsum in the strength development of fly ashes with lime. J Mater Civ Eng 23:197–206

Sridharan A (2014) Soil clay mineralogy and physico-chemical mechanisms governing the fine-grained soil behaviour. Indian Geotech J 44(4):371–339. https://doi.org/10.1007/s40098-014-0136-0

Sridharan A, Rao SM, Murthy NS (1988) Liquid limit of kaolinitic soils. Geotechnique 38(2):191–198

Sterpi D (2015) Effect of freeze–thaw cycles on the hydraulic conductivity of a compacted clayey silt and influence of the compaction energy. Soils Found 55(5):1326–1332

Van Jaarsveld JGS, Van Deventer JSJ, Lukey GC (2002) The effect of composition and temperature on the properties of fly-ash and kaolinite-based geopolymers. Chem Eng J 89:63–73

Wang SD, Scrivener KL, Pratt PL (1994) Factors affecting the strength of alkali activated slag. Cem, Concer, Res 24(6):1033–1043. https://doi.org/10.1016/0008-8846(94)90026-4

Wang S, Li L, Zhua ZH (2007) Solid-state conversion of fly ash to effective adsorbents for Cu removal from wastewater. J Hazard Mater 139(2):254–259. https://doi.org/10.1016/j.jhazmat.2006.06.018

Xu H, Van Deventer JSJ (2000) The geopolymerisation of aluminosilicate minerals. Int J Miner Process 59(3):247–266

Yilmaz G, Yetimoglu T, Arasan S (2008) Hydraulic conductivity of compacted clay liners permeated with inorganic salt solutions. Waste Manag Res 26(5):464–473

Zhang Y, Liu L (2013) Fly ash-based geopolymer as a novel photocatalyst for degradation of dye from wastewater. Particuology 11:353–358. https://doi.org/10.1016/j.partic.2012.10.007